Assessment of the "6-31+G** + LANL2DZ" Mixed Basis Set Coupled with Density Functional Theory Methods and the Effective Core Potential: Prediction of Heats of Formation and Ionization Potentials for First-Row-Transition-Metal Complexes

Yue Yang, Michael N. Weaver, and Kenneth M. Merz, Jr.*

Quantum Theory Project, Department of Chemistry, University of Florida, Gainesville, Florida 32611

Received: August 27, 2008; Revised Manuscript Received: July 18, 2009

Computational chemists have long demonstrated great interest in finding ways to reliably and accurately predict the molecular properties for transition-metal-containing complexes. This study is a continuation of our validation efforts of density functional theory (DFT) methods when applied to transition-metal-containing systems (Riley, K.E.; Merz, K. M., Jr. *J. Phys. Chem.* **2007**, *111*, 6044−6053). In our previous work we examined DFT using all-electron basis sets, but approaches incorporating effective core potentials (ECPs) are effective in reducing computational expense. With this in mind, our efforts were expanded to include evaluation of the performance of the basis set derived to approximate such an approach as well on the same set of density functionals. Indeed, employing an ECP basis such as LANL2DZ (Los Alamos National Laboratory 2 double ζ) for transition metals, while using all-electron basis sets for all other non-transition-metal atoms, has become more and more popular in computations on transition-metal-containing systems. In this study, we assess the performance of 12 different DFT functionals, from the GGA (generalized gradient approximation), hybrid-GGA, meta-GGA, and hybrid-meta-GGA classes, respectively, along with the 6-31+G** + LANL2DZ (on the transition metal) mixed basis set in predicting two important molecular properties, heats of formation and ionization potentials, for 94 and 58 systems containing first-row transition metals from Ti to Zn, which are all in the third row of the periodic table. An interesting note is that the inclusion of the exact exchange term in density functional methods generally increases the accuracy of ionization potential prediction for the hybrid-GGA methods but decreases the reliability of determining the heats of formation for transition-metal-containing complexes for all hybrid density functional methods. The hybrid-GGA functional B3LYP gives the best performance in predicting the ionization potentials, while the meta-GGA functional TPSSTPSS provides the most reliable and accurate results for heat of formation calculations. TPSSTPSS, a meta-GGA functional, which was constructed from first principles and subject to known exact constraints just like in an "ab initio" way, is successful in predicting both the ionization potentials and the heats of formation for transition-metal-containing systems.

1. Introduction

There has been growing interest in transition metals (TMs) and their complexes in computational chemistry because of not only the very important roles these elements play in modern chemistry[1] but also the well-known difficulties associated with their theoretical treatments.[2] The biggest problem associated with the calculation of TM-containing systems is the near degeneracy stemming from electrons partially occupying the d orbitals. Recently, several studies have been conducted to evaluate the performance of different density functional theory (DFT) methods for predicting several molecular properties and studying reactions involving TMs;[3,4] also several studies have been carried out to improve the performance of DFT functionals.[5,6] However, to obtain very accurate and reliable calculations for the TM-containing systems, one must implement multireference methods such as multireference configuration interaction (MRCI). Unfortunately, these kinds of methods are usually very expensive; therefore, as the interest in carrying out calculations for large systems (such as proteins) keeps growing,[7,8] identifying computational methods that are less expensive than multireference methods but still able to achieve good performance is desirable. DFT is a promising choice because it is able to efficiently predict the atomic and molecular properties for a variety of systems.[9,10] DFT has a great advantage over the Hartree−Fock (HF) method in describing electron correlation effects and has favorable scaling properties with respect to molecular size when compared to post-Hartree−Fock methods. As a result, DFT is a widely used computational approach for studying large TM-containing compounds and shows significant promise as an ab initio method that can be used to investigate large macromolecules such as proteins and DNA.

With the exact density functional unknown, DFT is actually a family of methods instead of a single method.[11] Most DFT methods are made up of a correlation functional, an exchange functional, and, in some cases, an exact exchange term in the same form as the HF exchange to approximate the exact density functionals. Some recently developed functionals also integrate terms that are functionally dependent on the kinetic energy density.[12,13] According to the types of functional dependencies that they possess, density functional methods can be divided into five well-known classes: LSDA, GGA, meta-GGA, hybrid-GGA, and hybrid-meta-GGA.[11] Among them, LSDA (the local spin density approximation) is the simplest type of density functional method as it is only dependent upon the electron density. GGA, the generalized gradient approximation, depends

* To whom correspondence should be addressed. E-mail: merz@qtp.ufl.edu.

10.1021/jp807643p CCC: $40.75
Published on Web 08/19/2009

TABLE 1: All the Functionals Employed in This Study[a]

type	functional	HF term proportion (%)	ref
GGA	BLYP	0	42, 43
GGA	MPWPW91	0	44−46
GGA	PBEPBE	0	47
hybrid-GGA	B3LYP	20	42, 43, 48, 49
hybrid-GGA	PBE1PBE	25	47, 50, 51
hybrid-GGA	B98	22	52
meta-GGA	TPSSTPSS	0	12, 13
meta-GGA	TPSSKCIS	0	12, 13, 53−55
meta-GGA	BB95	0	42, 56
hybrid-meta-GGA	B1B95	28	42, 56
hybrid-meta-GGA	TPSS1KCIS	13	12, 13, 53−55, 57
hybrid-meta-GGA	BB1K	42	42, 56, 58

[a] The third column gives the proportion of the exact exchange term in the exchange part of the functional.

not only on the electron density but also on its reduced gradient. Meta-GGA also depends upon the kinetic energy density. Hybrid-GGA and hybrid-meta-GGA are the combinations of GGA and meta-GGA with the HF exchange term, respectively. For this study, we have chosen to exclude LSDA and focus on the other four types of functionals, utilizing three of each variety.

Perdew and Schmidt have used a "Jacob's ladder" analogy to describe density functional approximations for the exchange-correlation energy as a function of the electron density.[11] Their Jacob's ladder scheme consists of five rungs with higher rungs (or levels) comprising more complex ingredients, thus providing more accurate approximations. The four classes of DFT methods considered in our study cover the second, third, and fourth rungs of Jacob's ladder. The hybrid-meta-GGA class is the most complex one included in this study, but is not the highest rung of Jacob's ladder, in which the functionals are supposed to have both an exact exchange term and an exact partial correlation term.[11,14] Although Perdew and co-workers have developed a fifth-rung functional by combining the exact exchange term and a second-order correlation term with a gradient-correlation density functional,[15,16] this type of functional is likely to be less widely used, supported by the fact that there were only a limited number of this class of functionals developed in the past several years. Therefore, we decided to not include functionals from the fifth rung in this study because we aim to assess the performance for the most widely used DFT methods. Also, because of some well-known issues such as difficulties in getting LSDA to converge properly and poor results given by LSDA for TMs,[17,18] we excluded the first-rung functionals as well. All of the DFT methods studied in this work are listed in Table 1, classified by the category to which each functional belongs.

In this work we employed the "6-31+G** + LANL2DZ" mixed basis set (denoted below as MBS) that utilizes the Los Alamos effective core potential on the transition metal, while utilizing a Pople-type basis set on all other atoms. The Pople-type split valence basis sets are extensively used in ab initio quantum chemistry calculations and, as a result, are well validated. In this study, we chose 6-31+G**, a double-ζ Pople-type basis set. LANL2DZ (Los Alamos National Laboratory 2 double-ζ), which is a widely used effective core potential (ECP)-type basis set, was used to model the metal atoms.[19] This mixed basis set was created through the use of the GEN keyword in Gaussian 03. Both of these basis sets have been widely used along with density functional methods for studies of TM-containing systems, and mixed basis sets of this type have been very popular in computational chemistry studies in this area in recent years.

With the chemically inactive core electrons represented by an ECP, the computational cost is decreased, since the cost formally increases as $\sim N^4$, where N is the number of explicitly treated electrons. In the past few years, many efforts have been made in generating a consistent set of ab initio ECPs and improving their quality to make the accuracy and reliability of ECP-based valence-electron calculations able to approach all-electron calculations.[19−23]

In this study, we evaluated the accuracy and reliability that can be expected from utilizing DFT functionals in calculating the heats of formation and ionization potentials for various systems containing first-row TMs. The ionization potential is defined as the energy that is required to remove an electron from a gaseous bound state to infinite separation. It is a measurement of the strength by which the electron is bound, an indicator of the reactivity of a substance and therefore an important property for atoms and molecules. The heat of formation, which by definition is the change in enthalpy that accompanies the formation of 1 mol of a substance in its ground state from its constituent elements in their most stable states, is a physical parameter used to measure the stability of a molecule and estimate other thermodynamic properties. The ability to predict these two physical properties is very important and has a significant impact on the fields of photoelectron spectroscopy, thermodynamics, and physical chemistry. In this study, 94 systems were used to assess the performance of DFT functionals in the prediction of the heats of formation and 58 systems were used to test their abilities to determine ionization potentials. All systems considered in this study, either atomic or molecular, contain first-row transition metals. As in our previous study by Riley and Merz,[24] we excluded scandium from our test because its experimental atomic enthalpy of formation is unavailable, which unfortunately is necessary to calculate the molecular heat of formation. All of the computational results are subjected to comparison to the most recent available experimental data to evaluate the performance of the density functional methods. Table 2 shows the experimental values of the heats of formation, and Table 3 gives the values of the ionization potentials.

Several studies have been carried out to assess the performance of density functional theory methods on predicting the properties of TM-containing systems within the past several years.[3,17,18,24−34] Recently, Riley and Merz have carried out several assessments to evaluate the performance of different DFT functionals from different "rungs" combined with different basis sets on computing the ionization potentials, heats of formation and other properties for systems containing first-row TMs.[24,26] Prior to that, Furche and Perdew utilized a quadruple-ζ quality basis set[35] assessing the performance of several different density functional methods for the description of properties including the bond energetics, molecular structures, dipole moments, and harmonic frequencies in 3d-TM-containing systems.[3] Cundari et al. evaluated the accuracy of heats of formation for molecules containing transition metals from the computations carried out by using the B3LYP functional paired with the effective-core-potential-based LANL2DZ and CEP-31G* basis sets.[36] An assessment using the B3LYP functional and ECP was made by Glukhovtsev, Bach, and Nagel; they employed an "in-house" pseudopotential-based basis set to study the bond dissociation energies, ionization potentials, enthalpies of formation, and harmonic frequencies of a set of iron-containing compounds.[28] Additionally, Amin and Truhlar recently studied zinc coordination compounds with O, S, NH_3, H_2O, OH, SCH_3, and H ligands; a large part of their work was focused on testing the predictions on Zn−ligand bond distances, dipole moments,

TABLE 2: Experimental Heats of Formation for All Systems Considered in This Work (kcal/mol)

TiH	116.4 ± 2.3[a]	MnH	64.2 ± 7.0[b]	Ni_2	156.7[l]
TiO	13.7 ± 2.2[b]	MnO	29.6 ± 3.0[b]	NiH	85.6 ± 2.6[b]
TiN	112.1 ± 2.3[b]	MnOH	3.7 ± 3.2[b]	NiO	75.0 ± 5.0[b]
TiF	−4.0 ± 8.0[b]	MnF	−19.9 ± 3.0[b]	NiF	17.5[b]
TiF_2	−164.5 ± 10.0[c,d]	MnF_2	−126.2 ± 1.0[b]	NiF_2	−77.8 ± 1.1[b]
TiF_3	−284.1 ± 10.0[c,d]	MnF_3	−188.0 ± 14.0[b]	NiCl	41.7 ± 1.6[l]
TiCl	24.2[b]	MnCl	11.3 ± 2.1[b]	$NiCl_2$	−17.4 ± 1.0[l]
$TiCl_2$	−57.0 ± 3.0[b]	$MnCl_2$	−63.0 ± 0.5[b,c]	NiS	81.7 ± 5.0[b]
$TiCl_3$	−128.9[c−e]	MnS	63.3 ± 2.0[b]	$Ni(OH)_2$	−60.8 ± 3.0[b]
TiS	76.2 ± 2.2[b]			NiCO	35.1 ± 5.8[j]
		Fe_2	172.4 ± 8.0[b]	$Ni(CO)_2$	−39.0 ± 2.5[j]
V_2	187.4 ± 5.2[b]	FeH	117.2 ± 1.0[f]	$Ni(CO)_3$	−92.7 ± 1.9[d]
VH	125.9 ± 2.0[f]	FeO	61.1 ± 3.0[b]	$Ni(CO)_4$	−144.0 ± 0.6[c,d]
VO	30.5[c,g]	FeF	11.4[d]		
VN	121.0 ± 3.0[b]	FeF_2	−93.0 ± 3.4[g]	Cu_2	113.8 ± 2.6[b]
VF	0.7 ± 15.0[b]	FeF_3	−196.2 ± 5.0[g]	CuH	65.9 ± 2.0[b]
VCl	37.8 ± 1.5[b]	FeCl	49.5 ± 1.6[k]	CuO	76.5 ± 10.0[b]
VCl_2	−51.6 ± 3.6[b]	$FeCl_2$	−32.8 ± 1.0[k]	CuOH	28.7 ± 4.0[b]
VCl_3	−88.2 ± 2.1[b]	$FeCl_3$	−60.6 ± 1.0[b]	CuCl	19.3 ± 2.0[b]
VS	80.4 ± 3.2[b]	FeS	83.8 ± 5.0[b]	$CuCl_2$	−9.0[m]
		$Fe(OH)_2$	−79.0 ± 0.5[g]	CuF	−3.2 ± 2.0[b]
CrH	80.2 ± 10.0[b]	Fe(CO)	63.9 ± 3.5[j]	CuF_2	−66.0[b]
CrO	45.0[c−e]	$Fe(CO)_2$	0.2 ± 4.9[j]	CuS	75.1 ± 5.0[b]
CrO_2	−18.0[c−e]	$Fe(CO)_3$	−55.8 ± 7.6[j]		
CrO_3	−70.5 ± 20.0[b]	$Fe(CO)_4$	−105.1 ± 3.4[d]	Zn_2	57.7 ± 1.5[b]
CrOH	18.9 ± 1.8[h]			ZnH	62.9 ± 0.5[b]
$Cr(OH)_2$	−78.1 ± 2.6[h]			ZnO	52.8 ± 0.9[b]
CrN	120.7[e,g]	CoH	110.7 ± 1.0[f]	ZnF_2	−118.9 ± 1.1[b]
CrF	3.1 ± 2.4[i]	CoO	74.0 ± 5.1[b]	ZnCl	6.5 ± 1.0[b]
CrF_2	−99.1 ± 4.2[b]	CoF_2	−87.5[b]	$ZnCl_2$	−63.5 ± 0.4[b]
CrF_3	−199.8 ± 3.4[h]	CoCl	50.3 ± 1.6[k]	ZnS	48.7 ± 3.0[b]
CrCl	31.0 ± 0.6[h]	$CoCl_2$	−22.6 ± 1.0[k]	$Zn(CH_3)$	26.0 ± 2.5[b]
$CrCl_2$	−28.1 ± 0.4[h]	$CoCl_3$	−39.1[c−e]	$Zn(CH_3)_2$	12.9 ± 2.0[b]
$CrCl_3$	−67.7 ± 1.5[h]				
CrS	78.2 ± 5.1[b]				

[a] Reference 59. [b] Reference 60. [c] Reference 61. [d] Reference 62. [e] Reference 63. [f] Reference 64. [g] Reference 65. [h] Reference 66. [i] Reference 67. [j] Reference 68. [k] Reference 69. [l] Reference 70. [m] Reference 32.

and bond dissociation energies of 39 density functionals paired with two different basis sets, for the purpose of nonrelativistic and relativistic DFT calculations, respectively.[37] Our present work is to extend the previous study by Riley et al.[24] to systematically study a series of TM-containing complexes with a consistent choice of density functional methods and a mixed basis set that utilizes pseudopotential-based basis sets on TMs and Pople-type split valence basis sets on all other atoms. Larger basis sets could be used and, indeed, should be used in cases where extreme accuracy is required, but pseudopotentials represent an economical and widely employed approach that deserves to be carefully validated. This is the goal of the present study.

2. Methods

All calculations carried out in this study were performed using the Gaussian 03 suite of programs.[38] The MOLDEN program[39] was used for preprocessing, structure modification, and post-processing analyses of structures, frequencies, and forces. Ionization potentials were calculated adiabatically. Heats of formation were calculated using the method specified in the "Thermochemistry in Gaussian" white paper available at http://www.gaussian.com/g_whitepap/thermo.htm. The experimental data for both the heats of formation and the ionization potentials were obtained from the *NIST Chemistry WebBook* at http://webbook.nist.gov/chemistry/.

As mentioned before, our main goal in this study is to evaluate the accuracy that we can expect from different DFT methods in predicting the heats of formation (HOFs) and ionization potentials (IPs) for TM-containing systems. To achieve this goal, the IPs and HOFs of two sets of small systems, which were selected because their experimental data are available and easy to access, were computed and all of the computational results were then compared to the values obtained directly from experiments. Because our ultimate goal is to estimate the performance of DFT methods for larger systems, which increases the computational cost significantly, we were only interested in standard methods, and therefore, only default grid sizes, convergence criteria, and optimization procedures have been employed in this study. This choice is easy to understand when one considers the tight connection between the extra or more expensive computational cost and the use of those special techniques, such as very fine grids and very tight convergence criteria. Further supporting this choice, Riley and Merz have reported that the finer grids and tighter convergence criteria had a limited effect on the results in most calculations from their tests.[24] Although it is popular to calculate the molecular properties at lower levels of theory by using the molecular geometries optimized at higher levels of theory, we optimized the molecular geometries and then calculated the IPs and HOFs using the same density functional method and basis set throughout this work. Once again, our expectation is that the results from this work will be able to inform future theoretical work on large systems such as metalloproteins.

It is well-known that DFT methods usually do not predict the same spin state as higher level methods such as MRCI. Therefore, we carried out the calculations of four different spin multiplicities for each of the systems considered in this study.

TABLE 3: Experimental Ionization Potentials for All Systems Studied in This Work (eV)

TiH	6[a]	$FeCl_2$	10.63± 0.10[c]
TiO	6.819 ± 0.006[a]	Fe(CO)	6.66 ± 0.17[d]
TiF_2	12.2 ± 0.5[a]	$Fe(CO)_2$	6.68 ± 0.24[d]
TiF_3	10.5 ± 0.5[a]	$Fe(CO)_3$	7.25 ± 0.35[d]
TiS	7.1 ± 0.3[a]	$Fe(CO)_4$	8.48[a]
V_2	6.357 ± 0.001[a]	CoH	7.86 ± 0.07[a]
VO	7.2386 ± 0.0006[a]	CoO	8.9 ± 0.2[a]
VN	8.0 ± 1.0[a]	CoCl	8.71 ± 0.10[c]
VS	8.4 ± 0.3[a]	$CoCl_2$	10.75 ± 0.10[c]
CrOH	7.54 ± 0.05[b]	NiH	8.50 ± 0.10[a]
CrO	8.16 ± 0.01[a]	NiO	9.5 ± 0.2[a]
CrO_2	10.3 ± 0.5[a]	NiF_2	11.5 ± 0.3[a]
CrO_3	11.6 ± 0.5[a]	NiCl	9.28 ± 0.10[c]
CrF	9.3 ± 0.4[a]	$NiCl_2$	11.24 ± 0.01[a]
CrF_2	10.6 ± 0.3[a]	Ni(CO)	7.30 ± 0.29[d]
CrF_3	12.5 ± 0.3[a]	$Ni(CO)_2$	7.79 ± 0.22[d]
CrCl	8.50 ± 0.10[c]	$Ni(CO)_3$	7.69 ± 0.25[d]
$CrCl_2$	9.9[a]	$Ni(CO)_4$	8.722 ± 0.010[a]
MnH	7.8[a]	Cu_2	7.9[a]
MnO	8.65 ± 0.20[a]	CuF	10.90 ± 0.01[a]
MnF	8.51 ± 0.20[a]	CuF_2	13.18[a]
MnF_2	11.38 ± 0.20[a]	CuCl	10.7 ± 0.3[a]
MnF_3	12.57 ± 0.20[a]		
MnCl	8.5 ± 0.3[c]	Zn_2	9.0 ± 0.2[a]
$MnCl_2$	11.03 ± 0.01[a]	ZnH	9.4[a]
Fe_2	6.3[a]	ZnO	9.34 ± 0.02[e]
FeO	8.9 ± 0.2[a]	ZnF_2	13.91 ± 0.03[a]
FeF_2	11.3 ± 0.3[a]	$ZnCl_2$	11.80 ± 0.005[a]
FeF_3	12.5 ± 0.3[a]	$Zn(CH_3)$	7.2[a]
FeCl	8.08 ± 0.10[c]	$Zn(CH_3)_2$	9.4[a]

[a] Reference 62. [b] Reference 69. [c] Reference 60. [d] Reference 67. [e] Reference 71. [f] Reference 68. [g] Reference 72. [h] Reference 73.

The rule is simple: 1, 3, 5, and 7 multiplicities for systems with odd numbers of electrons while multiplicities 2, 4, 6, and 8 for those systems with an even number of electrons are calculated (the iron dimer is an exception for which multiplicity 9 was also calculated). Only the spin state with the lowest electronic energy is chosen to further calculate both the HOFs and IPs (detailed information of calculated multiplicities for each system with all functionals is provided in the Supporting Information). A separate frequency calculation after geometry optimization is recommended for the hybrid-meta-GGA functionals BB1K and TPSS1KCIS, and further details can be found at http://comp.chem.umn.edu/info/DFT.htm. Although the Gaussian group suggests that the *stable* keyword be used to identify the ground state of TM-containing systems, we found it to be necessary to double check and make sure that the optimized structure corresponds to the ground state. Imaginary frequencies frequently appear on these flat potential energy surfaces, which can be corrected by making small geometric changes followed by geometry optimizations. It is also worth noting that all of the single-point energy calculations for atoms, which are required to compute the HOFs, were calculated using the SCF=*tight* keyword in Gaussian 03.

3. Results and Discussion

a. Heats of Formation. Each of 94 systems considered in our study were calculated with all 12 functionals paired with the MBS. The average unsigned errors for each of the functionals are given in Figure 1. The first insight of Figure 1 is that the first group of three functionals (GGA class) performs better than the second group (hybrid-GGA class) and the third group (meta-GGA class) outperforms the fourth group (hybrid-meta-GGA class). The best performance is given by functionals

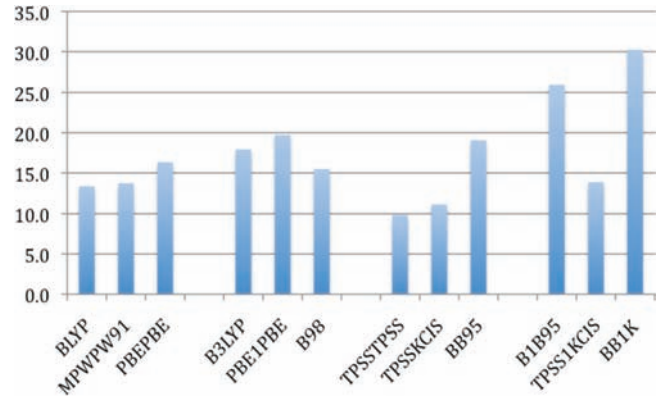

Figure 1. Average unsigned heat of formation errors for the entire set of systems containing transition metals considered in this study (kcal/mol).

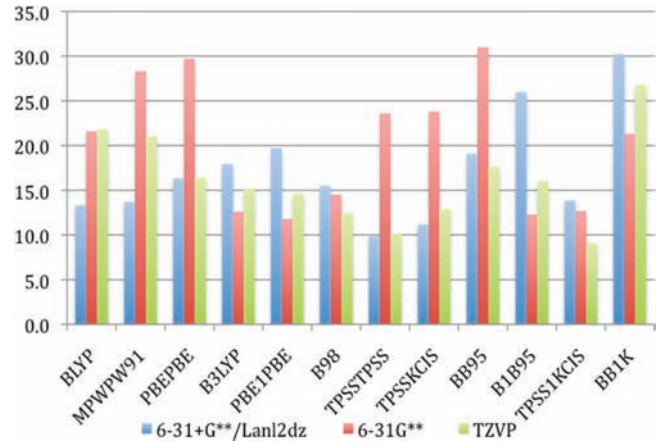

Figure 2. Average unsigned heat of formation errors for the entire set of transition-metal systems compared to the results of the 6-31G** and TZVP basis sets (kcal/mol).

TPSSTPSS and TPSSKCIS, which are both members of the meta-GGA family, and the 9.9 kcal/mol average unsigned error produced by TPSSTPSS is the lowest average error observed. On the other hand, the largest average errors come with functionals B1B95 and BB1K, both of which are from the hybrid-meta-GGA class. Despite the poor performance of others in the hybrid-meta-GGA class, TPSS1KCIS gives reasonably good results. Comparing the proportion of the exact exchange being included in the exchange term of the hybrid-meta-GGA methods (listed in Table 1), it seems that increasing the proportion of the HF term decreases the quality of the computed results.

To compare this new set of results to the previous results obtained by Riley and Merz,[24] we included both sets of results in Figure 2. It is encouraging to see that the MBS employed in this study outperforms both the 6-31G** and TZVP basis sets in 3 of 12 functionals by a significant margin and outperforms 6-31G** while giving results comparable to those of TZVP in another 3 of 12 functionals (i.e., in 6 out of 12 cases it outperforms all-electron 6-31G** calculations). It is interesting to note that all the hybrid-GGA and hybrid-meta-GGA functionals, which include the exact exchange, do not work that well with the MBS. Some of them, such as B1B95 and even B3LYP, produce much larger errors than either 6-31G** or TZVP. From these two figures, it is difficult to draw a definitive conclusion establishing the relationship between the functional class and the quality of the HOF results, but it seems that the integration of the exact exchange term does not improve the quality of the

TABLE 4: Average Unsigned Heat of Formation Errors for the Entire Set of Systems Containing Various Transition Metals (kcal/mol)

	Ti	V	Cr	Mn	Fe	Co	Ni	Cu	Zn	total
BLYP	16.0	16.2	10.5	10.9	20.3	14.5	9.0	8.8	13.0	13.3
MPWPW91	14.8	13.0	9.3	13.6	28.1	10.6	10.7	7.6	8.9	13.7
PBEPBE	13.8	12.9	9.5	32.1	30.6	13.9	14.0	7.0	7.9	16.3
B3LYP	16.6	25.1	16.9	9.4	19.4	19.8	25.2	13.5	12.7	17.9
PBE1PBE	18.4	30.1	25.5	24.2	13.7	17.9	24.0	13.5	8.7	19.7
B98	14.1	25.4	12.8	9.9	21.1	9.8	20.7	8.4	10.9	15.5
TPSSTPSS	12.6	12.2	6.0	9.8	16.0	9.2	8.3	6.3	6.3	9.9
TPSSKCIS	13.5	12.2	7.5	11.0	21.1	11.7	6.5	7.0	7.5	11.2
BB95	27.0	14.3	14.0	13.6	43.5	11.2	15.6	7.1	10.1	19.1
B1B95	33.6	33.3	34.6	41.3	19.8	21.7	23.2	14.4	10.3	26.0
TPSS1KCIS	13.9	21.7	15.7	6.0	12.2	16.7	18.4	11.3	7.9	13.9
BB1K	37.7	42.4	39.8	15.1	34.7	21.4	37.3	17.7	10.9	30.2

heats of formation with an ECP basis set. Some detailed analysis of Figure 2 and other figures or tables can be found in the Supporting Information.

Table 4 shows the average unsigned HOF errors (error = experiment − theory) for the entire set of systems containing various TMs treated in our study. Riley and Merz have reported that chromium, nickel, and copper were the most problematic TMs for the 6-31G** basis set,[24] but none of them are the most problematic TMs with MBS. Instead, in this study, copper gives the best average performance; zinc is another TM that gives an impressive performance, perhaps because of its closed shell electronic configuration. This time, vanadium and iron are the most problematic TM types. Going through this table horizontally, it is clear that the meta-GGA functionals TPSSTPSS and TPSSKCIS outperform all other functionals examined herein by a significant margin. The GGA functionals BLYP and MPWPW91, along with the hybrid-meta-GGA functional TPSS1KCIS, also give less than 15.0 kcal/mol average unsigned errors. TPSSTPSS, a member of the meta-GGA class, is the only one successfully giving average unsigned errors lower than 20.0 kcal/mol for each TM. Despite the good performance of TPSS1KCIS, the other two hybrid-meta-GGA functionals (B1B95 and BB1K) are really problematic when paired with the MBS. BB1K is the most disappointing functional, with six out of nine groups producing 30.0+ kcal/mol average unsigned errors and a total average of 30.2 kcal/mol. As a conclusion, iron-containing systems and the BB1K functional have the largest problems working with the MBS.

Table 5 gives the average signed error of the HOF calculation for systems containing various TMs treated in this study. Apparently, all the hybrid-GGA and hybrid-meta-GGA functionals tend to overestimate the HOF, and five of six GGA and meta-GGA methods underestimate the HOF, with the meta-GGA functional TPSSTPSS being the only exception. It is also worth noting that not a single functional underestimates all nine types of TM-containing systems while on the contrary three functionals (B3LYP, B98, and TPSS1KCIS) overestimate all nine types of TM-containing systems and the three other hybrid functionals overestimate eight of nine types of TM-containing systems. Another point deserving attention is that the HOFs for systems containing vanadium and zinc are overestimated by all 12 functionals studied in this work and the HOFs for systems containing titanium and copper are overestimated by at least 10 functionals, with PBEPBE being the only exception for both cases. It should not be ignored that only the manganese- and iron-containing systems have more than half of the functionals producing positive average signed HOF errors.

Table 6 exhibits the average unsigned HOF errors for all systems sorted by various TM-coordinating groups. It is clear that the TM oxides and carbonyl complexes give the poorest results, while the TM hydrides seem to be the most benign functional group in our study, and the TM sulfides and the hydroxides are reasonably well modeled. The meta-GGA functional TPSSTPSS once again gives the most outstanding performance in this study, and on the other hand, the incorporation of the exact exchange term still negatively impacts DFT's performance. Comparing our results with those obtained by Riley et al.,[24] it is encouraging to see that the maximum average unsigned error in this table (49.0 kcal/mol) is much smaller than the poorest result from both 6-31G** (84.4 kcal/mol) and TZVP (62.1 kcal/mol), and at the same time the minimum error (3.3 kcal/mol) is also lower than the best result from either 6-31G** (6.1 kcal/mol) or TZVP (5.5 kcal/mol).

Table 7 lists the average unsigned HOF errors for all the functionals considered in this study categorized by the number of coordinating groups associated with the TMs (please note that the transition-metal dimers are not included in this analysis). It is noteworthy that there is an obvious trend regarding the quality of the HOF prediction and the number of groups coordinating to the TMs: the average unsigned error grows significantly with increasing degree of coordination. In fact, 11 of 12 functionals considered in this study follow this trend, with the hybrid-meta-GGA functional B1B95 being the only exception. Notably, for the monocoordinated systems, all functionals but BB1K give a good performance. The effect of incorporating the exact exchange term is shown clearly in the sets of dicoordinate and tricoordinate systems if one compares the results from nonhybrid functionals to those from hybrid functionals. For tetracoordinate systems, only TPSSTPSS produces average unsigned errors lower than 20.0 kcal/mol. Perhaps this trend to larger errors as a function of coordination results from functional designs based on mono- or dicoordinate metal species. If this is the case, higher coordinate species need to be taken into account in future functional designs.

It is useful to compare our results with those previously generated in our laboratory and reported by Riley et al.[24,26] In Riley's first study,[26] a variety of density functional methods were paired with the 6-31G* basis set to evaluate their performance on several atomic or molecular properties for standard organic compounds, while in Riley's more recent TM study,[24] another Pople-type basis set, 6-31G**, was paired with 12 density functional methods; in our study, the only change we made to Riley's second study is the basis set: an ECP-type basis set was utilized for all TM atoms with 6-31+G** for the remaining atoms. It was found that, with the change of the basis set, the performance of the GGA class functionals improves dramatically with an average of 10.0+ kcal/mol better than those with 6-31G** and also an average of about 5.0 kcal/mol better than those with TZVP. Also, it was noticed that although the incorporation of the exact exchange term improves DFT's performance for both organic compounds and TM-containing systems in the previous studies, troubles arise with the MBS used in our study. With the decreased performance from hybrid density functional methods, it is not surprising to see that the meta-GGA functionals TPSSTPSS and TPSSKCIS became the most reliable DFT methods in our study, although they still do not reach the level of accuracy that DFT methods provide for standard organic compounds. It will be interesting to see what DFT methods can do using the D(T)ZVP/LANL2DZ or LANL2TZ[20] basis set in the future.

b. Ionization Potentials. Figure 3 shows the average unsigned ionization potential errors for all 58 TM-containing compounds included in our study. A quick scan of the figure shows that B3LYP outperforms the other 11 functionals while

TABLE 5: Average Signed Heat of Formation Error for the Entire Set of Systems Containing Various Transition Metals (kcal/mol)

	Ti	V	Cr	Mn	Fe	Co	Ni	Cu	Zn	total
BLYP	−2.7	−5.7	4.9	4.5	14.3	6.1	−4.8	−2.3	−12.7	0.2
MPWPW91	−2.6	−7.6	1.3	11.1	25.9	1.2	5.7	−0.9	−6.7	3.0
PBEPBE	0.6	−5.0	4.3	32.1	29.2	13.7	11.0	0.7	−5.1	9.1
B3LYP	−13.1	−22.4	−16.1	−9.1	−17.3	−15.4	−25.2	−12.2	−12.7	−15.9
PBE1PBE	−16.6	−29.0	−25.4	24.2	−7.3	−14.5	−24.0	−12.9	−8.7	−12.7
B98	−11.1	−25.4	−11.6	−9.9	−17.3	−9.8	−20.7	−6.2	−10.9	−13.7
TPSSTPSS	−3.9	−9.1	−3.2	8.2	12.4	2.9	−4.5	−1.0	−3.6	−0.2
TPSSKCIS	−2.7	−7.6	−0.7	8.9	17.7	10.1	0.1	−1.7	−5.5	2.1
BB95	−10.2	−5.9	2.3	1.1	24.1	7.3	12.9	1.0	−6.9	2.9
B1B95	−32.8	−33.3	−34.5	38.7	−18.2	−17.2	−23.2	−13.6	−10.3	−16.0
TPSS1KCIS	−11.9	−19.6	−15.0	−1.4	−7.5	−11.7	−18.4	−10.2	−7.2	−11.4
BB1K	−37.7	−42.4	−39.8	−15.1	32.5	−17.9	−37.3	−17.7	−10.9	−20.7

TABLE 6: Average Unsigned Heat of Formation Errors for Various Transition-Metal-Coordinating Groups[a] (kcal/mol)

	no.	BLYP	MPWPW91	PBEPBE	B3LYP	PBE1PBE	B98	TPSSTPSS	TPSSKCIS	BB95	B1B95	TPSS1KCIS	BB1K	av
MDs	5	13.5	13.0	14.6	17.4	22.0	18.5	11.2	11.5	19.8	23.8	13.5	29.2	17.3
H	9	10.1	9.2	10.7	10.6	9.3	7.2	9.7	10.2	10.8	10.9	9.1	17.2	10.4
N	3	16.6	12.3	15.5	13.9	23.5	8.8	3.3	9.3	18.5	23.1	10.2	37.6	16.1
O	11	16.6	16.0	21.3	16.7	24.4	14.2	7.9	12.1	21.1	39.1	12.6	47.1	20.8
S	8	9.1	10.2	12.9	12.5	14.6	15.3	8.8	9.4	12.0	20.7	8.9	24.2	13.2
F	19	10.2	10.8	13.8	13.7	19.5	12.2	10.7	10.8	25.4	32.3	13.4	31.1	17.0
Cl	23	16.0	12.1	11.3	22.1	19.9	17.3	10.0	10.4	11.0	21.2	16.6	25.9	16.2
OH	6	6.9	9.1	12.1	12.0	20.7	14.5	9.6	8.7	8.6	30.0	14.7	21.3	14.0
CO	8	17.0	34.8	45.7	36.8	27.6	29.6	13.6	17.9	49.0	29.9	20.2	45.2	30.6
CH_3	2	25.7	15.1	11.3	20.5	15.5	20.1	8.9	12.8	17.2	19.6	14.0	20.1	16.7

[a] "MDs" denotes metal dimers, and "no." refers to the number of examples of a particular coordinating group within the test set.

TABLE 7: Unsigned Heat of Formation Errors for Transition-Metal Complexes Based on the Number of Coordinating Groups Present[a] (kcal/mol)

	no.	BLYP	MPWPW91	PBEPBE	B3LYP	PBE1PBE	B98	TPSSTPSS	TPSSKCIS	BB95	B1B95	TPSS1KCIS	BB1K	av
1	51	11.6	11.5	14.6	10.9	13.6	10.0	8.5	10.3	13.7	17.5	8.4	22.6	12.7
2	24	14.4	13.9	14.7	20.5	21.9	17.0	10.3	11.2	15.2	29.8	17.2	31.8	18.2
3	12	17.0	18.3	20.0	36.0	36.5	29.2	13.0	13.3	41.8	51.4	27.5	55.3	29.9
4	2	22.0	43.4	61.1	60.3	44.8	48.2	17.7	21.1	64.0	48.6	33.5	59.3	43.7

[a] "no." refers to the number of examples for each case; please note that metal dimers are omitted in this analysis.

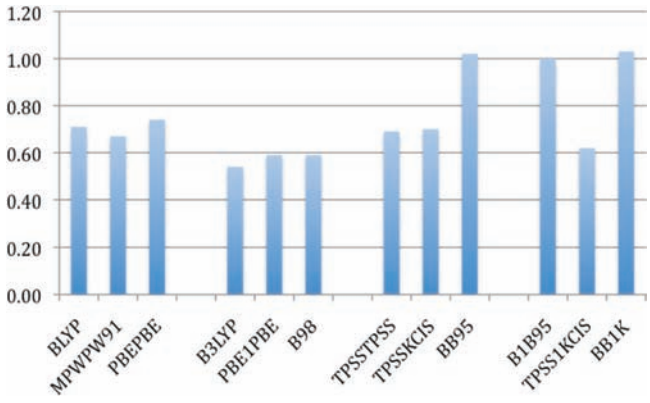

Figure 3. Average unsigned ionization potential errors for the entire set of transition-metal-containing systems treated in this work (eV).

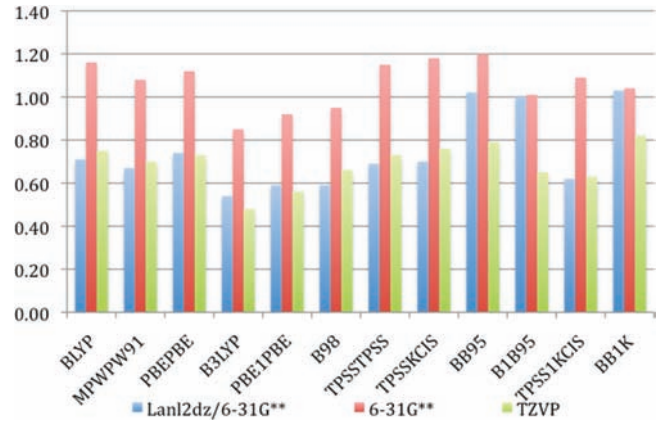

Figure 4. Average unsigned ionization potential errors for the entire set of transition-metal-containing systems compared to the results from Riley and Merz[24] (eV).

the hybrid-GGA outperforms the other three classes of functionals. Unlike in HOF calculations where the incorporation of the exact exchange term decreases the accuracy for hybrid density functional methods, there is no obvious tendency in our IP assessment: on one hand, the hybrid-GGA leads all other classes, while on the other hand, the hybrid-meta-GGA becomes the most disappointing class again. It is also interesting to see that within the same class there is no significant difference between functionals except the poor performance of BB95 in the meta-GGA class and the solid performance of TPSS1KCIS in the hybrid-meta-GGA class.

Also, we compared our average unsigned errors with the results from a previous DFT assessment by Riley and Merz[24] and summarize the comparison in Figure 4. Clearly, the MBS outperforms 6-31G** and gives results comparable to those the TZVP set. Taking an 0.8 eV error as a qualitative benchmark level that separates good from bad performance, one finds that all 12 functionals paired with the 6-31G** basis set produce average unsigned errors above this level. BB95 and two hybrid-meta-GGA methods (B1B95 and BB1K) paired with MBS give

TABLE 8: Average Unsigned Ionization Potential Errors for the Entire Set of Transition-Metal Systems Considered in This Study (eV)

	Ti	V	Cr	Mn	Fe	Co	Ni	Cu	Zn	total
BLYP	1.38	0.45	0.67	0.82	0.49	0.43	0.44	0.58	1.19	0.71
MPWPW91	1.39	0.42	0.57	0.77	0.47	0.46	0.47	0.51	1.10	0.67
PBEPBE	1.40	0.43	0.59	0.80	0.48	0.34	0.83	0.54	1.13	0.74
B3LYP	1.24	0.56	0.42	0.51	0.25	0.78	0.36	0.28	0.83	0.54
PBE1PBE	1.23	0.58	0.47	0.46	0.46	0.69	0.37	0.42	0.96	0.59
B98	1.14	0.90	0.49	0.52	0.47	0.30	0.36	0.34	1.01	0.59
TPSSTPSS	1.40	0.48	0.64	0.80	0.38	0.48	0.38	0.69	1.22	0.69
TPSSKCIS	1.39	0.49	0.66	0.83	0.39	0.45	0.40	0.66	1.24	0.70
BB95	1.57	0.73	0.97	1.37	1.17	0.96	0.63	0.34	1.19	1.02
B1B95	3.32	0.84	1.12	1.12	0.49	0.43	0.44	0.58	1.19	1.00
TPSS1KCIS	1.19	0.61	0.49	0.65	0.25	0.85	0.34	0.59	1.15	0.62
BB1K	2.37	0.83	0.56	0.98	0.96	0.76	0.73	1.43	1.21	1.03

errors above 0.8 eV, while only BB1K paired with TZVP gives an error higher than this level. Although in our study the hybrid-GGA class outperforms the other three, its performance is not that impressive when compared with the TZVP test. The best performance of a specific functional for all basis sets belongs to B3LYP, which partially explains why it is one of the most popular DFT methods at present. On the other hand, BB1K gives the poorest performance when paired with MBS and TZVP and gives very poor results when paired with 6-31G**.

The average unsigned ionization potential errors for all TM-containing systems included in this study are shown in Table 8. Clearly, the titanium-containing systems yielded the worst performance, and zinc-containing systems were troublesome when using the MBS. Iron and nickel performed better in this test, which is opposite to what was observed in the HOF study. The best individual performance comes from TPSS1KCIS and B3LYP both on iron (0.25 and 0.26 eV), while the poorest performance belongs to B1B95 on titanium (3.32 eV). Looking at the average performance by functionals, B3LYP is the clear leader (0.54 eV), with BB1K being the worst (1.03 eV). There are two other functionals (B1B95 and BB1K) producing no lower than 1.00 eV average unsigned errors. Coincidently, both of them incorporate Becke's 88 exchange functional and Becke's 95 correlation functional like BB1K does, with the proportion of the exchange functional in each method being the only difference.

Table 9 gives the average signed ionization potential errors for all nine groups of TM-containing systems. These results match the tendency seen previously by Riley and Merz[24] which showed that DFT methods generally underestimated IP using either the 6-31G** or TZVP basis set. Table 9 has many more entries with negative signs than those of Riley and Merz[24] (zero for 6-31G** and four for TZVP), but still much fewer than the entries that are underestimated. Nickel and cobalt are the only two TMs that have more overestimated entries than underestimated entries. BB1K gives the best overall performance in this comparison, but this is misleading because it gives both large under- and overestimated results, which tend to cancel one another out. By excluding BB1K, B3LYP gives the lowest average signed error over all functionals (0.29 eV), which again shows its strength in predicting IPs.

Table 10 gives the average unsigned ionization potential errors for all TM-containing systems classified by different coordinating environments. TM fluorides give the biggest troubles in this table. Although it seems that the hybrid-GGA methods have an advantage in IP prediction, there is a different tendency in TM nitrides where hybrid DFT methods produce larger average unsigned errors than their corresponding nonhybrid DFT brethren. TM hydroxides appear to give the best performance, but there is only one sample from this group being tested by each functional. TM oxides and TM chlorides are also well modeled, and this has been proved through testing a number of examples. Though TM hydrides and TM systems containing methyl groups give errors in an acceptable range, it seems that some improvement is warranted to get errors into the few tenths of an electronvolt range. Studying the table vertically, it is not surprising to see that all three hybrid-GGA functionals give

TABLE 9: Average Signed Ionization Potential Errors for the Entire Set of Transition-Metal-Containing Systems (eV)

	Ti	V	Cr	Mn	Fe	Co	Ni	Cu	Zn	total
BLYP	0.90	0.38	0.65	0.75	0.10	−0.01	−0.13	0.53	1.19	0.46
MPWPW91	0.88	0.30	0.52	0.66	0.02	−0.09	−0.25	0.48	1.10	0.38
PBEPBE	0.90	0.32	0.57	0.70	0.06	0.06	−0.56	0.51	1.13	0.36
B3LYP	0.64	0.44	0.30	0.37	0.08	−0.15	−0.03	0.27	0.83	0.29
PBE1PBE	0.76	0.51	0.32	0.34	0.08	−0.01	0.13	0.42	0.96	0.36
B98	1.02	0.05	0.29	0.52	0.21	0.11	0.09	0.34	1.01	0.39
TPSSTPSS	0.99	0.45	0.64	0.74	0.18	0.07	−0.09	0.69	1.22	0.51
TPSSKCIS	0.98	0.45	0.66	0.77	0.17	0.05	−0.08	0.66	1.24	0.52
BB95	1.25	0.73	0.69	1.13	0.56	−0.55	−0.30	0.22	1.19	0.56
B1B95	−0.82	0.84	0.51	0.57	0.10	−0.01	−0.13	0.53	1.19	0.31
TPSS1KCIS	1.00	0.58	0.46	0.60	0.22	0.12	0.12	0.59	1.15	0.51
BB1K	−2.37	0.81	−0.24	−0.25	0.19	−0.68	0.39	−1.10	0.52	−0.18

TABLE 10: Average Unsigned Ionization Potential Errors for Various Transition-Metal Bonding Partners[a] (eV)

	no.	BLYP	MPWPW91	PBEPBE	B3LYP	PBE1PBE	B98	TPSSTPSS	TPSSKCIS	BB95	B1B95	TPSS1KCIS	BB1K	av
MDs	4	0.48	0.50	0.50	0.45	0.90	0.48	0.56	0.55	0.51	0.52	0.66	1.34	0.62
H	5	0.94	0.99	0.91	0.96	0.90	0.64	0.93	0.93	0.95	0.94	0.87	0.72	0.89
N	1	0.79	0.73	0.74	1.14	1.20	1.70	0.93	0.92	0.91	1.31	1.37	1.29	1.09
O	10	0.27	0.28	0.28	0.36	0.42	0.37	0.32	0.31	0.63	1.23	0.40	1.01	0.49
S	2	0.46	0.38	0.39	0.40	0.39	0.64	0.43	0.45	0.55	1.26	0.39	0.59	0.53
F	14	1.17	1.10	1.15	0.79	0.82	0.89	1.19	1.20	1.96	1.42	0.97	1.58	1.19
Cl	12	0.62	0.52	0.54	0.36	0.35	0.38	0.53	0.56	0.70	0.71	0.47	0.55	0.52
OH	1	0.11	0.02	0.02	0.20	0.20	0.82	0.15	0.14	1.25	1.29	0.12	1.02	0.45
CO	8	0.61	0.68	1.06	0.36	0.45	0.48	0.51	0.51	0.77	0.61	0.33	1.00	0.61
CH_3	2	0.87	0.71	0.74	0.61	0.61	0.70	0.81	0.85	0.85	0.87	0.78	0.63	0.75

[a] "MDs" denotes metal dimers, and "no." refers to the number of examples of a particular bonding partner within the test set.

TABLE 11: Average Unsigned Ionization Potential Errors for Transition-Metal Complexes Based on the Number of Coordinating Groups Present[a] (eV)

	no.	BLYP	MPWPW91	PBEPBE	B3LYP	PBE1PBE	B98	TPSSTPSS	TPSSKCIS	BB95	B1B95	TPSS1KCIS	BB1K	av
1	29	0.49	0.48	0.58	0.53	0.55	0.57	0.51	0.51	0.72	0.76	0.54	0.94	0.60
2	17	1.01	0.92	0.96	0.58	0.61	0.66	0.93	0.96	0.82	1.28	0.75	0.75	0.85
3	7	1.02	1.03	1.07	0.36	0.40	0.38	0.98	1.01	3.19	1.72	0.56	1.72	1.12
4	2	0.58	0.48	0.47	1.09	1.17	1.32	0.53	0.51	0.43	0.58	0.82	1.54	0.79

[a] "no." refers to the number of examples for each case; please note that metal dimers are omitted in this analysis.

consistently good performance over all liganding groups (except for TM nitrides where only one data point was available). BB95 and all three hybrid-meta-GGA functionals are still struggling to predict IPs for TM-containing systems when the MBS is used.

Table 11 shows the average unsigned ionization potentials errors for all TM-containing systems examined in this study as a function of the number of coordinating groups associated with the transition metal (again, transition-metal dimers are not included in this analysis). Interestingly, there are several different trends observed in this table: (1) for all the hybrid-GGA functionals, the lowest average errors are obtained from tricoordinated systems, while the errors for others tend to increase with increasing coordination; (2) for all the GGA and meta-GGA functionals, the increasing error with increasing coordination is not a constant, but a variable; (3) for the hybrid-meta-GGA methods, no clear trend is apparent because each one seems to have its own trend. We note that for monocoordinated systems the difference between the remaining functionals is quite small (0.58−0.48 eV) if one ignores BB95, B1B95, and BB1K. It is also clear that the hybrid-GGA methods dominate the others for tricoordinate species while, on the other hand, they perform poorly for tetracoordinate species, but further work will be needed to verify the latter case since only two experimental data points were used to reach this conclusion.

Once again, it is of interest to compare the IP study with that of Riley et al.[24,26] Obviously most DFT functionals paired with MBS do a better job than with 6-31G**. Our error ranges (0.54−1.03 eV) are much better than that with 6-31G** (0.85−1.20 eV), although there is a long way to go to reach the error bars seen for organic compounds (0.25−0.35 eV) using the 6-31G* basis set. B3LYP is absolutely the most reliable DFT method in IP studies no matter whether it is paired with 6-31G* for organic systems or with 6-31G** or MBS for TM-containing systems.

4. Conclusions

Comparing the ground-state spin multiplicities predicted by different functionals paired with the MBS, it is found that most functionals' predictions agree with one another with the exception of B1B95 along with BB1K differing from the remaining 10 functionals. For most functionals, the favored spin multiplicities are in good agreement regardless of the basis set choice, while for B1B95 and BB1K there are numerous differences between MBS and 6-31G** or TZVP. This fact alone likely accounts for the relatively poor performance given by these two hybrid-meta-GGA methods. Moreover, we find that the predicted spin multiplicities given by MBS match those given by TZVP more often than with the 6-31G** basis set.

The GGA and meta-GGA classes of functionals generally produce better results than the hybrid-GGA and hybrid-meta-GGA functionals in predicting HOFs. We find that the meta-GGA method TPSSTPSS has a better performance than other methods, producing the lowest average unsigned error of 10.3 kcal/mol, less than 16.0 kcal/mol errors for each type of TM-containing system, less than 14.0 kcal/mol errors for each of the 10 TM-coordinating ligands, and less than 18.0 kcal/mol errors for each of the four coordination modes. TPSSKCIS, another meta-GGA functional that also employs the TPSS exchange functional but uses the KCIS instead of TPSS correlation functional, provides a solid performance with the MBS as well. The dramatic change between this study and the previous one is the greatly improved performance by the GGA class of functionals which turns one of the most troublesome approaches by Riley and Merz into one of the better approaches. In contrast to Riley and Merz,[24] we find that B1B95 is less trustworthy along with BB1K.

The hybrid-GGA class proves its dominance in predicting IPs, with all three class members giving average unsigned errors no higher than 0.58 eV, which is 0.10 eV better than the best result from other functionals. However, unlike the previous study where integration of the exact exchange term improved the performance of IP prediction, the inclusion of the exact exchange term seems to have a limited effect on the hybrid-meta-GGA methods. We find that the meta-GGA methods (except BB95) give results comparable to those of the GGA functionals; the parametrization not working well with ionized systems might be the reason that this type of functional does not show as impressive an improvement as it shows in the HOF study. B3LYP gives the best performance in the present study with a 0.54 eV average unsigned error and errors lower than 0.85 eV for all types of TM systems except Ti (1.24 eV). BB95, B1B95, and BB1K perform relatively poorly, with each of them producing average signed errors above 1.00 eV.

The present study unearthed both encouraging and disappointing results. The positive points are (1) the MBS HOF performance of the GGA and hybrid-GGA methods is much improved over that of 6-31G** and in some instances even better than that of TZVP and (2) the IP errors of nine functionals (except BB95, B1B95, and BB1K) are much better than those with 6-31G** and are at least comparable to those with TZVP. The negative points are (1) the more advanced functionals from the hybrid-meta-GGA class except TPSS1KCIS failed to give an improved performance and (2) the HOF and IP results are still not comparable to the results for standard organic systems.

The study of TMs and their complexes is still a significant challenge in computational chemistry, and much work remains to further create and validate quantum mechanical methods suitable for the study of TMs. Trying more advanced DFT functionals and larger basis sets may not be as helpful as hoped because the improvement in theory does not necessarily translate into improved models. This is highlighted by the observation that "advanced" DFT methods such as the hybrid-meta-GGA functionals did not provide us with more accurate results; instead, simpler methods such as the GGA functionals performed well sometimes. Friesner and co-workers have described a localized orbital model in which an ex post facto correction is applied;[40,41] this approach is certainly helpful, but we believe that having an accurate "base" quantum chemical model is also

an important goal to pursue. Therefore, to accomplish the community goal of accurate TM modeling, experimental efforts are clearly necessary as are more sophisticated electronic structure methods that can provide both accurate thermochemical data and accurate electronic structure. We are pursuing the latter in earnest in ongoing efforts in our laboratory.

Acknowledgment. We thank the NIH (Grants GM066859 and GM044974) for providing the funding for this research. M.N.W. thanks the NIH for support in the form of an NRSA postdoctoral fellowship (Grant F32GM079968).

Supporting Information Available: Additional information, including data for all heat of formation and ionization potential calculations. This material is available free of charge via the Internet at http://pubs.acs.org.

References and Notes

(1) Cotton, F. A.; Wilkinson, G.; Murillo, C. A. *Advanced Inorganic Chemistry*; Wiley: New York, 1999.
(2) Austin, I. G.; Mott, N. F. *Science* **1970**, *168*, 71.
(3) Furche, F.; Perdew, J. P. *J. Chem. Phys.* **2006**, *124*, 044103.
(4) Quintal, M. M.; Karton, A.; Iron, M. A.; Boese, A. D.; Martin, J. M. L. *J. Phys. Chem. A* **2006**, *110*, 709.
(5) Brown, S. T.; Kong, J. *Chem. Phys. Lett.* **2005**, *408*, 395.
(6) Li, H.; Shi, L.; Zhang, M.; Su, Z.; Wang, X.; Hu, L.; Chen, G. *J. Chem. Phys.* **2007**, *126*, 144101.
(7) Gogonea, V.; Suarez, D.; van der Vaart, A.; Merz, K. W. *Curr. Opin. Struct. Biol.* **2001**, *11*, 217.
(8) Sousa, S. F.; Fernandes, P. A.; Ramos, M. J. *J. Am. Chem. Soc.* **2007**, *129*, 1378.
(9) Hohenberg, P.; Kohn, W. *Phys. Rev.* **1964**, *136B*, 864.
(10) Kohn, W.; Sham, L. J. *Phys. Rev.* **1965**, *140A*, 1133.
(11) Perdew, J. P.; Schmidt, K. *AIP Conference Proceedings*; AIP: Melville, NY, 2001; Vol. 577, pp 1−20.
(12) Tao, J.; Perdew, J. P.; Staroverov, V. N.; Scuseria, G. E. *Phys. Rev. Lett.* **2003**, *91*, 146401.
(13) Staroverov, V. N.; Scuseria, G. E.; Tao, J.; Perdew, J. P. *J. Chem. Phys.* **2003**, *119*, 12129.
(14) Mattsson, A. E. *Science* **2002**, *298*, 759.
(15) Seidl, M.; Perdew, J. P.; Kurth, S. *Phys. Rev. A* **2000**, *62*, 012502.
(16) Seidl, M.; Perdew, J. P.; Kurth, S. *Phys. Rev. Lett.* **2000**, *84*, 5070.
(17) Görling, A.; Trickey, S. B.; Gisdakis, P.; Rösch, N. *Topics in Organometallic Chemistry*; Springer: Berlin, 1999; Vol. 4, p 109.
(18) Schultz, N. E.; Zhao, Y.; Truhlar, D. G. *J. Phys. Chem. A* **2005**, *109*, 11127.
(19) Hay, P. J.; Wadt, W. R. *J. Chem. Phys.* **1985**, *82*, 299.
(20) Roy, L. E.; Hay, P. J.; Martin, R. L. *J. Chem. Theory Comput.* **2008**, *4*, 1029.
(21) Hay, P. J.; Wadt, W. R. *J. Chem. Phys.* **1985**, *82*, 270.
(22) Wadt, W. R.; Hay, P. J. *J. Chem. Phys.* **1985**, *82*, 284.
(23) Lovallo, C. C.; Klobukowski, M. *J. Comput. Chem.* **2003**, *24*, 1009.
(24) Riley, K. E.; Merz, K. M., Jr. *J. Phys. Chem. A* **2007**, *111*, 6044.
(25) Schwarz, W. H. E.; Wang, S. G.; Scheurer, P. *Abstr. Pap.—Am. Chem. Soc.* **2000**, *220*, U501.
(26) Riley, K. E.; Holt, B. T. O.; Merz, K. M., Jr. *J. Chem. Theory Comput.* **2007**, *3*, 407.
(27) Cundari, T. R.; Leza, H. A. R.; Grimes, T.; Steyl, G.; Waters, A.; Wilson, A. K. *Chem. Phys. Lett.* **2004**, *401*, 58.
(28) Glukhovtsev, M. N.; Bach, R. D.; Nagel, C. J. *J. Phys. Chem. A* **1997**, *101*, 316.
(29) Bach, R. D.; Shobe, D. S.; Schlegel, H. B. *J. Phys. Chem.* **1996**, *100*, 8770.
(30) Barone, V.; Adamo, C. *Int. J. Quantum Chem.* **1997**, *61*, 443.
(31) Barone, V.; Adamo, C.; Mele, F. *Chem. Phys. Lett.* **1996**, *249*, 290.
(32) Wang, S. G.; Schwarz, W. H. E. *J. Chem. Phys.* **1998**, *109*, 7252.
(33) Schultz, N. E.; Zhao, Y.; Truhlar, D. G. *J. Phys. Chem. A* **2005**, *109*, 4388.
(34) Zhao, Y.; Truhlar, D. G. *J. Chem. Phys.* **2006**, *124*, 224105.
(35) Weigend, F.; Furche, F.; Ahlrichs, R. *J. Chem. Phys.* **2003**, *119*, 12753.
(36) Cundari, T. R.; Leza, H. A. R.; Grimes, T.; Steyl, G.; Waters, A.; Wilson, A. K. *Chem. Phys. Lett.* **2005**, *401*, 58.
(37) Amin, E. A.; Truhlar, D. G. *J. Chem. Theory Comput.* **2008**, *4*, 75.
(38) Frisch, M. J.; Trucks, G. W.; Schlegel, H. B.; Scuseria, G. E.; Robb, M. A.; Cheeseman, J. R.; Montgomery, Jr., J. A.; Vreven, T.; Kudin, K. N.; Burant, J. C.; Millam, J. M.; Iyengar, S. S.; Tomasi, J.; Barone, V.; Mennucci, B.; Cossi, M.; Scalmani, G.; Rega, N.; Petersson, G. A.; Nakatsuji, H.; Hada, M.; Ehara, M.; Toyota, K.; Fukuda, R.; Hasegawa, J.; Ishida, M.; Nakajima, T.; Honda, Y.; Kitao, O.; Nakai, H.; Klene, M.; Li, X.; Knox, J. E.; Hratchian, H. P.; Cross, J. B.; Bakken, V.; Adamo, C.; Jaramillo, J.; Gomperts, R.; Stratmann, R. E.; Yazyev, O.; Austin, A. J.; Cammi, R.; Pomelli, C.; Ochterski, J. W.; Ayala, P. Y.; Morokuma, K.; Voth, G. A.; Salvador, P.; Dannenberg, J. J.; Zakrzewski, V. G.; Dapprich, S.; Daniels, A. D.; Strain, M. C.; Farkas, O.; Malick, D. K.; Rabuck, A. D.; Raghavachari, K.; Foresman, J. B.; Ortiz, J. V.; Cui, Q.; Baboul, A. G.; Clifford, S.; Cioslowski, J.; Stefanov, B. B.; Liu, G.; Liashenko, A.; Piskorz, P.; Komaromi, I.; Martin, R. L.; Fox, D. J.; Keith, T.; Al-Laham, M. A.; Peng, C. Y.; Nanayakkara, A.; Challacombe, M.; Gill, P. M. W.; Johnson, B.; Chen, W.; Wong, M. W.; Gonzalez, C.; Pople, J. A., Gaussian, Inc., Wallingford, CT, 2004.
(39) Schaftenaar, G.; Noordik, J. H. *J. Comput.-Aided Mol. Des.* **2000**, *14*, 123.
(40) Friesner, R. A.; Knoll, E. H.; Cao, Y. *J. Chem. Phys.* **2006**, *125*, 124107.
(41) Knoll, E. H.; Richard, A. F. *J. Phys. Chem. B* **2006**, *110*, 18787.
(42) Becke, A. D. *Phys. Rev. A* **1988**, *38*, 3098.
(43) Lee, C.; Yang, W.; Parr, R. G. *Phys. Rev. B* **1988**, *37*, 785.
(44) Perdew, J. P.; Chevary, J. A.; Vosko, S. H.; Jackson, K. A.; Pederson, M. R.; Singh, D. J.; Fiolhais, C. *Phys. Rev. B* **1992**, *46*, 6671.
(45) Perdew, J. P.; Wang, Y. *Phys. Rev. B* **1992**, *45*, 13244.
(46) Adamo, C.; Barone, V. *J. Chem. Phys.* **1998**, *108*, 664.
(47) Perdew, J. P.; Burke, K.; Ernzerhof, M. *Phys. Rev. Lett.* **1996**, *77*, 3865.
(48) Stephens, P. J.; Devlin, F. J.; Chabalowski, C. F.; Frisch, M. J. *J. Phys. Chem.* **1994**, *98*, 11623.
(49) Hertwig, R. H.; Koch, W. *Chem. Phys. Lett.* **1997**, *268*, 345.
(50) Adamo, C.; Barone, V. *Chem. Phys. Lett.* **1998**, *298*, 113.
(51) Adamo, C.; Barone, V. *J. Chem. Phys.* **1999**, *110*, 6158.
(52) Schmider, H. L.; Becke, A. D. *J. Chem. Phys.* **1998**, *108*, 9624.
(53) Rey, J.; Savin, A. *Int. J. Quantum Chem.* **1998**, *69*, 581.
(54) Krieger, J. B.; Chen, J.; Iafrate, G. J.; Savin, A. In *Electron Correlations and Materials Properties*; Gonis, A., Kioussis, N., Eds.; Plenum: New York, 1999; p 463.
(55) Toulouse, J.; Savin, A.; Adamo, C. *J. Chem. Phys.* **2002**, *117*, 10465.
(56) Becke, A. D. *J. Chem. Phys.* **1996**, *104*, 1040.
(57) Zhao, Y.; Lynch, B. J.; Truhlar, D. G. *Phys. Chem. Chem. Phys.* **2005**, *7*, 43.
(58) Zhao, Y.; Lynch, B. J.; Truhlar, D. G. *J. Phys. Chem. A* **2004**, *108*, 2715.
(59) Chen, Y.-M.; Clemmer, D. E.; Armentrout, P. B. *J. Chem. Phys.* **1991**, *95*, 1063.
(60) Yungman, V. S., Ed. *Thermal Constants of Substances*; Wiley: New York, 1999; Vols. *4*−*6*.
(61) Barin, I. *Thermochemical Data of Pure Substances*; VCH: Weinheim, Germany, 1989.
(62) Mallard, W. G.; Linstrom, P. J. *NIST Chemistry WebBook: NIST Standard Reference Database Number 69*; National Institute of Standards and Technology: Gaitherburg, MD, 2000.
(63) Binnewies, M.; Milke, E. *Thermochemical Data of Elements and Compounds*; Wiley-VCH: Weinheim, Germany, 1999.
(64) Barone, V.; Adamo, C. *Int. J. Quantum Chem.* **1997**, *61*, 443.
(65) Chase, M. W.; Davies, C. A.; Downey, J. R.; Frurip, D. J.; McDonald, R. A.; Syverud, A. N. *JANAF Thermochemical Tables*, 3rd ed.; 1985; Vol. 14, Suppl. 1.
(66) Ebbinghaus, B. B. *Combust. Flame* **1995**, *101*, 311.
(67) Espelid, O.; Borve, K. J. *J. Phys. Chem. A* **1997**, *101*, 9449.
(68) Sunderlin, L. S.; Wang, D.; Squires, R. R. *J. Am. Chem. Soc.* **1992**, *114*, 2788.
(69) Hildenbrand, D. L.; Lau, K. H. *J. Chem. Phys.* **1995**, *102*, 3769.
(70) Morse, M. D. *Chem. Rev.* **1986**, *86*, 1049.
(71) Rohlfing, E. A.; Cox, D. M.; Kaldor, A.; Johnson, K. H. *J. Chem. Phys.* **1984**, *81*, 3846.
(72) Lide, D. *CRC Handbook of Chemistry and Physics*; CRC: Boca Raton, FL, 1991.
(73) Clemmer, D. E.; Dalleska, N. F.; Armentrout, P. B. *J. Chem. Phys.* **1991**, *95*, 7263.

JP807643P